

Differential effects of cocaine on histone posttranslational modifications in identified populations of striatal neurons

Emmanuelle Jordi^{a,b,c,d}, Myriam Heiman^{d,1}, Lucile Marion-Poll^{b,c}, Pierre Guermonprez^e, Shuk Kei Cheng^d, Angus C. Nairn^{d,f}, Paul Greengard^{d,2}, and Jean-Antoine Girault^{a,b,c,2}

^aUnité Mixte de Recherche en Santé 839, Institut National de la Santé et de la Recherche Médicale, 75005 Paris, France; ^bUniversité Pierre et Marie Curie, 75005 Paris, France; ^cInstitut du Fer à Moulin, 75005 Paris, France; ^dLaboratory of Molecular and Cellular Neuroscience and ^eLaboratory of Molecular Immunology, The Rockefeller University, New York, NY 10065; and ^fDepartment of Psychiatry, Yale School of Medicine, Yale University, New Haven, CT 06508

Contributed by Paul Greengard, April 17, 2013 (sent for review March 6, 2013)

Drugs of abuse, such as cocaine, induce changes in gene expression and epigenetic marks including alterations in histone posttranslational modifications in striatal neurons. These changes are thought to participate in physiological memory mechanisms and to be critical for long-term behavioral alterations. However, the striatum is composed of multiple cell types, including two distinct populations of medium-sized spiny neurons, and little is known concerning the cell-type specificity of epigenetic modifications. To address this question we used bacterial artificial chromosome transgenic mice, which express EGFP fused to the N-terminus of the large subunit ribosomal protein L10a driven by the D1 or D2 dopamine receptor (D1R, D2R) promoter, respectively. Fluorescence in nucleoli was used to sort nuclei from D1R- or D2R-expressing neurons and to quantify by flow cytometry the cocaine-induced changes in histone acetylation and methylation specifically in these two types of nuclei. The two populations of medium-sized spiny neurons displayed different patterns of histone modifications 15 min or 24 h after a single injection of cocaine or 24 h after seven daily injections. In particular, acetylation of histone 3 on Lys 14 and of histone 4 on Lys 5 and 12, and methylation of histone 3 on Lys 9 exhibited distinct and persistent changes in the two cell types. Our data provide insights into the differential epigenetic responses to cocaine in D1R- and D2R-positive neurons and their potential regulation, which may participate in the persistent effects of cocaine in these neurons. The method described should have general utility for studying nuclear modifications in different types of neuronal or nonneuronal cell types.

addiction | psychostimulant drugs | chromatin | nucleus | fluorescence-activated cell sorting

In both humans and rodents, repeated self-administration of addictive substances can lead to a state of addiction characterized by a loss of control over drug use, with compulsive self-administration despite its severe negative consequences (1). The addictive state is persistent, with drug craving and relapse occurring even after decades of abstinence. All addictive drugs share the ability to increase extracellular dopamine (DA) levels in the ventral striatum (2) and are thought to exert their long-lasting effects by “hijacking” the normal reward systems, including the mesolimbic-striatal DA pathway and the nucleus accumbens (NAc) (3–5).

A single exposure to psychostimulants triggers long-lasting alterations in behavior and synaptic physiology (6), revealing their powerful control of neuronal plasticity. Repeated exposures induce further changes that contribute to the occurrence of addiction (7–10). Growing evidence suggests that long-lasting changes in the properties of striatal neurons involve epigenetic processes (11). In particular, histone posttranslational modifications (PTMs), including phosphorylation, acetylation, and methylation play a role in promoting transcriptional alterations following cocaine administration (12, 13). Acute exposure to cocaine induces rapid changes in histone phosphorylation and acetylation through

a variety of signaling pathways activated downstream from DA and glutamate receptors (14). Moreover, repeated cocaine administration regulates histone-modifying enzymes in the NAc, including histone deacetylases, acetyltransferases, and methyltransferases (15).

The striatum is composed of multiple cell types, which exhibit different transcriptional responses to drugs of abuse and mediate distinct aspects of addiction (16). Most (95% in rodents) striatal neurons are GABAergic medium-sized spiny neurons (MSNs), which can be further differentiated into D1 DA receptor- (D1R)- and D2R-expressing neurons, broadly corresponding to neurons of the direct (striatonigral) and indirect (striatopallidal) pathways, respectively (17). Each population of MSNs expresses its own subset of markers and has different projections (18). Cocaine-induced signaling cascades (19, 20) and transcriptional regulation (21) are strikingly different in the two types of MSNs. Cocaine-induced histone H3 serine-10 phosphorylation occurs in D1 but not in D2 neurons (20); however, little is known about other potential differences in histone modification in these two populations.

Here we have developed a unique approach, taking advantage of the specific labeling of the two types of MSNs by expressing EGFP fused to the N-terminus of ribosome large subunit protein L10a (EGFP-L10a) under the control of the D1R or D2R promoters in transgenic mice (21). The high enrichment of EGFP-L10a in nucleoli allows fluorescence-activated counting and sorting of nuclei (22). Using flow cytometry, we studied cocaine-induced histone PTMs in the two populations of MSNs separately. We found some similarities and many differences between the two populations, with distinct temporal regulations that are likely linked to specific patterns of gene expression.

Results

Fluorescence-Activated Purification of Nuclei in *Drd1a::EGFP-L10a* and *Drd2::EGFP-L10a* Transgenic Mice. We used bacterial artificial chromosome- (BAC)-transgenic mice, which express the EGFP-L10a fusion protein under the control of either the D1R or D2R promoter (DA receptor 1a, *Drd1a*, or 2, *Drd2*) promoter (21). The L10a protein is a component of the large subunit of the ribosome and allows the immune affinity purification of translating ribosomes (21). Because ribosomal subunits are assembled in the

Author contributions: E.J., M.H., P. Guermonprez, A.C.N., P. Greengard, and J.-A.G. designed research; E.J., L.M.-P., and S.K.C. performed research; E.J., L.M.-P., A.C.N., P. Greengard, and J.-A.G. analyzed data; and E.J., M.H., A.C.N., P. Greengard, and J.-A.G. wrote the paper.

The authors declare no conflict of interest.

¹Present address: Department of Brain and Cognitive Sciences, Picower Institute of Learning and Memory, Broad Institute of Massachusetts Institute of Technology and Harvard, Cambridge, MA 02142.

²To whom correspondence may be addressed. E-mail: jean-antoine.girault@inserm.fr or greengard@rockefeller.edu.

This article contains supporting information online at www.pnas.org/lookup/suppl/doi:10.1073/pnas.1307116110/-DCSupplemental.

nucleoli before being exported to the cytoplasm, the nuclei of D1R- or D2R-expressing neurons (from here on referred to as D1 or D2 nuclei) are intensely fluorescent for EGFP-L10a in these transgenic mice, as previously reported for other types of neurons (22) and can be isolated by fluorescence-activated sorting. Striata were dissected from the transgenic mice, and after homogenization and fixation (*Experimental Procedures*), nuclei were collected by subcellular fractionation and analyzed by flow cytometry (Fig. 1 *A* and *B*). The nuclei were also labeled with DyeCycle ruby (DCR), an intercalating dye that binds quantitatively to DNA. The dot plots allowed the distinction of several populations of nuclei according to the intensity of EGFP and DCR fluorescence. The majority of nuclei displayed a DNA fluorescence corresponding to single nuclei (singlets). Debris and aggregates were excluded from the analysis and only the EGFP-fluorescent singlets were considered (Fig. 1*B*). The total amount of GFP-positive singlets isolated was $16.4\% \pm 1.1\%$ and $7.1\% \pm 0.7\%$ of the total number of nuclei counted by the cytometer from the *Drd1a::EGFP-L10a* and mice *Drd2::EGFP-L10a*, respectively ($n = 18$ experiments, means \pm SEM). FACS-purified nuclei were examined by flow imaging (Fig. 1*C*) to verify they were intact, correctly sorted, and pure.

Histone Modifications in D1 and D2 Nuclei. In initial studies, we validated the FACS approach to isolate specific populations of nuclei and we assessed the stability of PTMs during the isolation procedure. Using immunoblotting of sorted nuclei, we examined

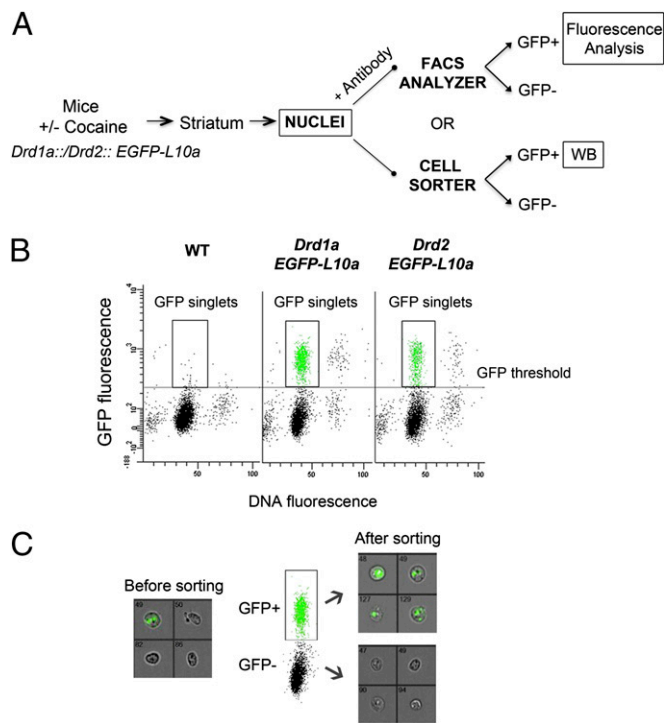


Fig. 1. Fluorescence-activated sorting of nuclei from *Drd1a::EGFP-L10a* and *Drd2::EGFP-L10a* transgenic mice. (*A*) Outline of the procedure used to study histone PTMs in isolated neuronal nuclei populations. Histone PTM changes were either quantified using immunolabeling of permeabilized nuclei (+ antibody) and flow cytometry or using immunoblotting of sorted D1 and D2 nuclei (WB). (*B*) Typical flow cytometry dot plot and gating of D1 or D2 nuclei. Scatterplot of GFP fluorescence versus DyeCycle ruby (DCR) fluorescence of nuclei isolated from a WT mouse and *Drd1a::EGFP-L10a* or *Drd2::EGFP-L10a* transgenic mice. DCR binds quantitatively to the DNA and allows discrimination of singlets versus aggregated nuclei. The data from WT mice were used to set a threshold for the GFP signal background. (*C*) After sorting, nuclei are pure and intact as verified by Amnis ImageStream analysis. Representative results are for pre- and postsort fractions from *Drd1a::EGFP-L10a* mice. Bright-field and GFP channels are merged; original magnification 40 \times .

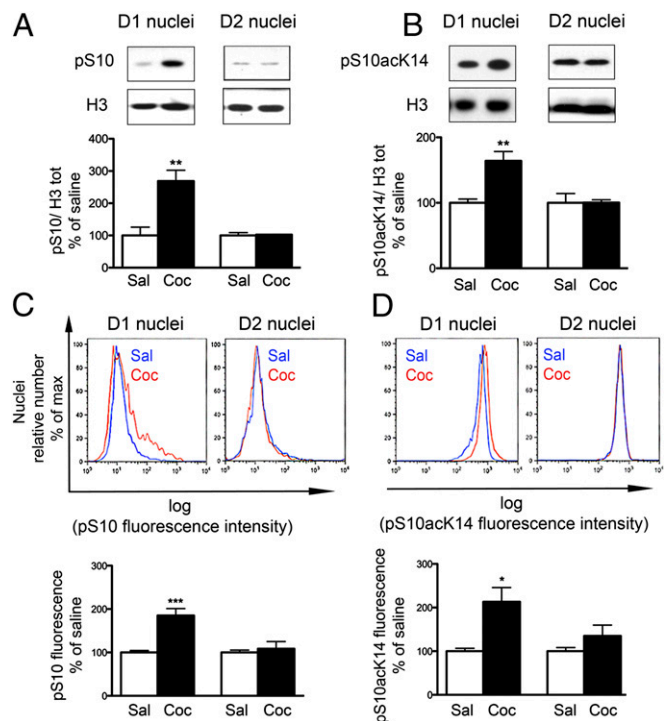


Fig. 2. Comparison of cocaine-induced histone H3 phosphorylation by immunoblotting of sorted nuclei and nuclear flow cytometry. Mice expressing EGFP-L10a in D1 or D2 neurons were treated with saline or cocaine (20 mg/kg) 15 min before tissue collection. (*A* and *B*) Immunoblot analysis of phospho-Ser10 H3 (pS₁₀, *A*) or phospho-Ser10 acetyl-Lys14 H3 (pS₁₀acK₁₄, *B*) in lysates from fluorescence-activated sorted D1 or D2 nuclei. All results were normalized to the total level of H3. (*Upper*) Representative blots obtained using antibodies against pS₁₀H3, pS₁₀acK₁₄H3, and total H3. (*Lower*) Quantification as percentage of saline-treated controls, mean \pm SEM ($n = 5-8$; $**P < 0.01$ Student *t* test). (*C* and *D*) Flow cytometry analysis of pS₁₀H3 (*C*) or pS₁₀acK₁₄H3 (*D*) immunofluorescence in the singlet GFP-positive nuclei corresponding to D1 or D2 nuclei. The logarithm of the fluorescence intensity is plotted on the *x* axis and relative nuclei number (percentage of maximum) on the *y* axis. (*Upper*) Representative flow cytometry histograms after saline (blue line) or cocaine (red line) treatment. (*Lower*) Quantification of flow cytometry data as percentage of saline-treated controls, mean \pm SEM ($n = 8-9$; $*P < 0.05$, $***P < 0.001$, Student *t* test).

the phosphorylation state of histone H3 Ser₁₀ (pS₁₀H3) alone or in combination with acetylation of K₁₄ (pS₁₀acK₁₄H3). After a single injection of cocaine or repeated injections, these two modifications have previously been shown to be induced in MSNs expressing the D1R, but not in those expressing the D2R (20). In the present study, nuclei were prepared from striata of EGFP-L10a mice, 15 min following a single injection of cocaine (20 mg/kg) or vehicle (saline). D1 or D2 nuclei were isolated by FACS and the levels of pS₁₀H3 and pS₁₀acK₁₄H3 were analyzed by immunoblotting. As expected, we observed a robust cocaine-induced increase in phosphorylation and in phosphoacetylation of H3 in D1 nuclei, but no change in the D2 nuclei (Fig. 2 *A* and *B*).

We carried out an analogous experiment but quantified the changes in pS₁₀H3 and pS₁₀acK₁₄H3 using immunolabeling of permeabilized nuclei combined with the use of a flow cytometer. The semilogarithmic plot of the number of immunoreactive, GFP-labeled nuclei as a function of the intensity of the immunofluorescence was rightward shifted for both pS₁₀H3 and pS₁₀acK₁₄H3 in the D1 nuclei after cocaine treatment (Fig. 2 *C* and *D*, *Upper*). Comparison of the semilogarithmic plots shows that cocaine causes the appearance of a small number of highly fluorescent D1 nuclei for pS₁₀H3 and a small magnitude, homogenous increase in pS₁₀acK₁₄H3 immunoreactivity, illustrating the sensitivity of the method. The pS₁₀H3 and pS₁₀acK₁₄H3

fluorescence quantified as the percentage of the mean of the fluorescence in the saline samples was increased in D1 nuclei (Fig. 2 C and D, Lower). In contrast, in the D2 nuclei, cocaine did not induce any significant change (Fig. 2 C and D).

Thus, flow cytometry gave results similar to those obtained by FACS followed by immunoblotting and could be used to measure histone PTMs in identified nuclear populations. Furthermore, these results show that cocaine-induced changes in phosphorylation are preserved during the procedure that appeared suitable to study other PTMs, such as acetylation and methylation, which are presumably as labile as or less labile than phosphorylation.

Differential Effects of Acute and Chronic Cocaine on Histone Acetylation in D1 and D2 Nuclei. Histone acetylation is considered to be a marker of actively transcribed genes and acute and chronic cocaine administrations induce histone acetylation in the striatum (14, 23, 24). Global acetylation of histones H3 and H4 has been investigated by the use of polyacetylated lysine antibodies, whereas other studies have focused on specific gene promoters using chromatin immunoprecipitation (12, 13, 25), but little is known concerning the regulation of acetylation of specific histone residues in identified neuronal cell types in the striatum. We first examined the nuclear localization of the acetylated forms of H3 on K₁₄ and K₁₈ and of H4 on K₅, K₈, and K₁₂ in striatal neurons by confocal microscopy of brain sections (Fig. 3, Left). The immunofluorescence was mostly colocalized with euchromatin, in support of the proposed role of these acetylated residues in gene activation (26). Given the high levels of immunoreactivity in saline-treated mice, we could not observe reliable quantitative changes after cocaine using tissue sections. We therefore examined the acetylation changes in D1 and D2 nuclei 15 min after a single injection of cocaine using flow cytometry. A single injection of cocaine rapidly increased to various extents acetylation of all studied lysine residues (H3 K₁₄ and K₁₈ and H4 K₅, K₈, and K₁₂) in D1 nuclei (Fig. 4A). The effect was much more pronounced for H4 K₅ (approximately threefold increase) than for the other residues (less than twofold, Fig. 4A). In contrast, in D2 nuclei, only H4 K₅ acetylation was

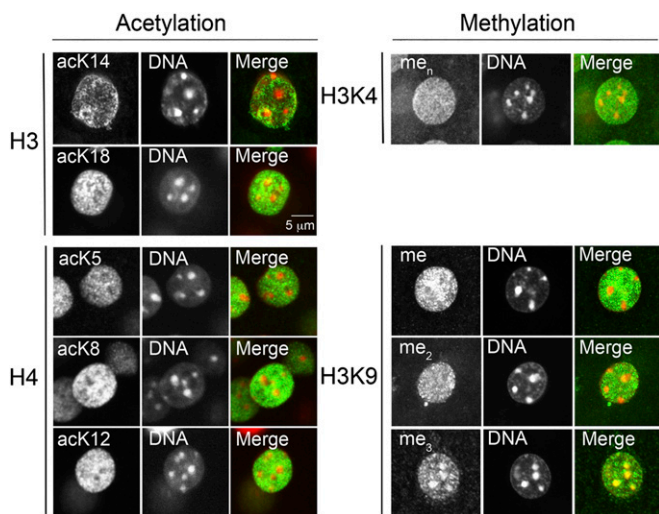


Fig. 3. Immunolocalization of histone PTMs in the nuclei of MSNs. Immunolocalization of histone acetylation (Left) including H3 acetyl-lysine14 (acK₁₄) and acetyl-lysine18 (acK₁₈), H4 acetyl-lysine5 (acK₅), acetyl-lysine8 (acK₈), and acetyl-lysine12 (acK₁₂) and histone H3 methylation (Right) including lysine4 (H3K4) methylation (me₁) and lysine9 (H3K9) mono-methylation (me), dimethylation (me₂), and trimethylation (me₃). DNA stained with DAPI (Center) and merged images (Right) are shown. Intense DAPI staining in large puncta corresponds to heterochromatin (usually less actively transcribed). (Scale bar, 5 μm.)

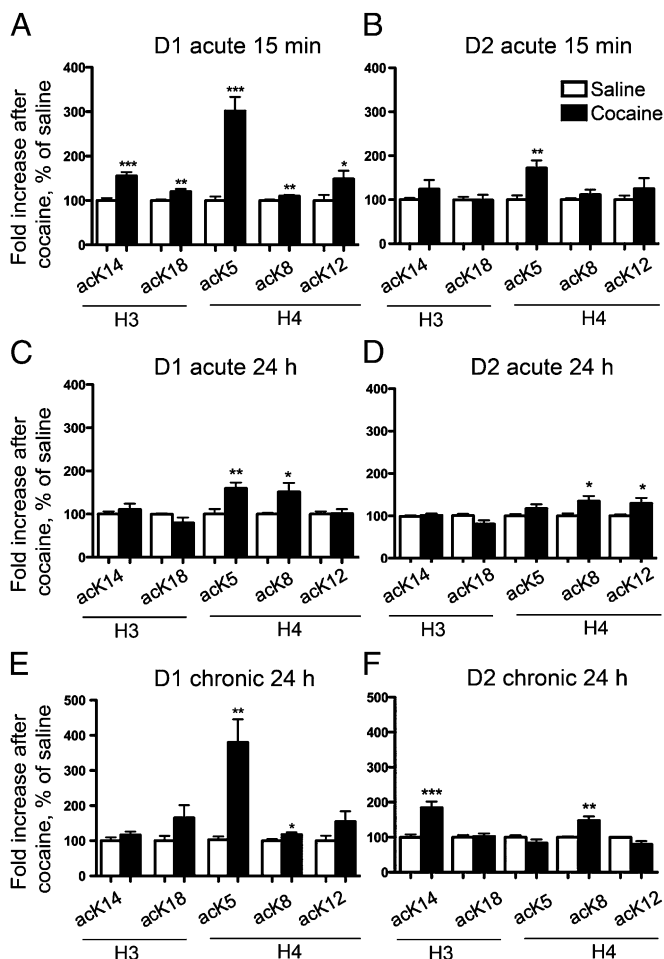


Fig. 4. Acute and chronic cocaine administration induces distinct patterns of histone H3 and H4 acetylation in D1 and D2 nuclei. Flow cytometry analysis of H3 acetyl-lysine14 (acK₁₄) and acetyl-lysine18 (acK₁₈), and of H4 acetyl-lysine5 (acK₅), acetyl-lysine8 (acK₈), and acetyl-lysine12 (acK₁₂) fluorescence in the GFP-positive nuclear fraction from D1 (A, C, and E) or D2 (B, D, and F) neurons. EGFP-L10a mice were injected with saline or cocaine (20 mg/kg) and killed 15 min (A and B) or 24 h (C and D) later. Other mice received a daily injection of 20 mg/kg cocaine or saline for 7 d and were killed 24 h after the last injection (E and F). Quantification of flow cytometry data are represented as percentage of saline-treated controls, mean + SEM ($n = 8-14$; * $P < 0.05$, ** $P < 0.01$, *** $P < 0.001$, Student t test).

moderately increased (Fig. 4B). Our data are consistent with the global increase in acK₅H4 immunofluorescence in striatal sections, measured 30 min after a cocaine injection (14).

Because these changes were observed at 15 min, we evaluated their stability 24 h later. A significant increase in H4 K₅ and K₈ acetylation was still observed in these conditions in D1 nuclei (Fig. 4C) showing the persistence of this histone modification specifically in the D1 nuclei. We also observed a moderate increase in H4 K₁₂ and K₈ acetylation in the D2 nuclei (Fig. 4D). Interestingly, H4 K₈ displayed a larger increase at 24 h than at 15 min in both cell types (Fig. 4C and D). These data show that a single injection of cocaine induces sustained acetylation of specific residues that are different in D1 and D2 MSNs.

We next investigated the effects of repeated cocaine injections on lysine acetylation, 24 h after the last injection. In D1 nuclei a strong increase (more than threefold) in H4 K₅ acetylation was observed, whereas the acetylation of other residues was either unchanged or very moderately increased (Fig. 4E). Interestingly, the effects of repeated treatment with cocaine were different in D2 nuclei, which displayed an increase in H3

K₁₄ and K₈ acetylation (Fig. 4*F*). These data show that repeated cocaine administration resulted in persistent histone acetylation patterns that were in part different from those observed after a single injection.

Flow Cytometry Reveals Subsets of D1 and D2 Nuclei with Different Levels of Histone Acetylation. Flow cytometry allows a quantitative analysis of heterogeneous samples providing a detailed profile of complex cells or nuclei populations that cannot be obtained with other methods such as immunoblotting. Whereas the results shown in Fig. 3 were based on comparison of mean fluorescence values, the analysis of the distribution of the fluorescence intensity showed that acK₅H4 immunofluorescence was not homogeneously distributed in control (saline treated) mice, but that two populations of nuclei were identifiable with low and high fluorescence intensity (typical patterns shown in Fig. 5*A, Left*). A similar bimodal distribution of acK₅H4 immunofluorescence was observed in the D1 and D2 nuclei from the various groups of saline-treated mice (Fig. 5*B* and Fig. S1, *Left*). This bimodal distribution was not observed, however, for pS₁₀H3 or pS₁₀acK₁₄H3 in saline-treated mice (Fig. 2 *C* and *D, Upper*). Following acute or repeated cocaine injections, the distribution of fluorescence in D1 nuclei was dramatically altered, with a shift toward a single population of highly fluorescent nuclei (Fig. 5*A* and Fig. S1*A, Center and Right*). A similar change was observed in D2 nuclei from acutely cocaine-treated mice (Fig. 5*B, Right*). In contrast, in D2 nuclei from mice treated with chronic cocaine, the pattern was heterogeneous and the two populations were not consistently changed compared with saline-treated mice (Fig. S1*B, Center and Right*), in agreement with the lack of increase in total fluorescence (Fig. 4*D*). These results indicate that MSNs are divided in two populations with different levels of K₅H4 acetylation. Cocaine treatment changes this distribution with a shift towards high acetylation.

D1 and D2 Nuclei Display Opposite Profiles of Histone H3 Methylation After Acute and Chronic Cocaine. Although considered to be relatively stable, histone methylation is emerging as a target for complex regulation (27). Histone methylation has been correlated with either gene activation (e.g., me₂K₄H3 and meK₉H3) or repression (me₂/me₃K₉H3) (28). Recent work has demonstrated that cocaine-regulated histone methylation in the striatum is associated with changes in gene transcription (13, 29), but it is not known in which cell type this posttranslational modification takes place. Interestingly, the immunoreactivity for these various methylations was differentially localized in MSN nuclei (Fig. 3, *Right*). meK₉ immunoreactivity was largely colocalized with euchromatin, whereas me₃K₉ labeling was predominantly

found in heterochromatin, consistent with their respective correlation with transcriptional activation and repression (28). me₂K₉ and me_nK₄H3 (where *n* can be 1-3) immunoreactivity was observed in both euchromatin and heterochromatin.

We then examined the effects of a single injection of cocaine on these four methylated marks. Cocaine induced rapid and robust changes in histone methylation as early as 15 min after a single injection of cocaine. In D1 nuclei H3 K₉ trimethylation was increased (Fig. 6*A*), whereas in D2 nuclei, the three methylated forms of H3 K₉ were increased (Fig. 6*B*). In both types of nuclei, methylation of H3 K₄ was unchanged (Fig. 6*A* and *B*). A day after a single injection of cocaine, me₂K₉ was persistently increased in D1 nuclei, whereas me₂K₉ and me_nK₄ were also significantly augmented by cocaine (Fig. 6*C*). In contrast, in D2 nuclei, methylation appeared to be more transient except for me₃K₉H3 (Fig. 6*D*).

Interestingly, the predominance of histone methylation changes in D1 over D2 nuclei was even more pronounced 24 h after the last of seven daily injections of cocaine. The three methylated forms of H3 K₉ were increased in D1 nuclei (Fig. 6*E*), whereas in D2 nuclei no significant difference between cocaine-treated and saline-treated mice was observed (Fig. 6*F*). These results show that the levels of H3 K₉ methylation are dynamically and differentially altered in D1 and D2 nuclei in response to cocaine and that these alterations are exclusively persistent in the D1 nuclei.

Discussion

To gain better insight into the cell-type-specific epigenetic marks induced by cocaine, we validated a fluorescence-activated flow cytometry procedure for isolating specific neuronal nuclei and rapidly and quantitatively analyzing histone PTMs. We showed that genetically labeled nuclei of D1R- and D2R-expressing neurons were intact and pure after FACS sorting and that labile cocaine-induced histone phosphorylation was preserved during the procedure. We then used flow cytometry to study histone PTMs in immunolabeled nuclei. This approach revealed the time-dependent cellular specificity of cocaine effects on histone acetylation and methylation in D1 and D2 nuclei.

The use of FACS in neuroscience provides a high-throughput means to study the phenotypic and functional heterogeneity of brain cells but is hampered by the intricate cell processes and interactions. Cells with few processes, such as those in embryonic tissues, and synaptosomes have been sorted with some success (30–32). More recently, adult neurons have been isolated by FACS, taking advantage of genetically encoded fluorescent probes, and used for gene expression profiling studies (33, 34). However, the entangled nature of mature neurons makes it difficult to separate cells without causing cellular damage or death. In addition, the difficulty and duration of the procedure used to dissociate

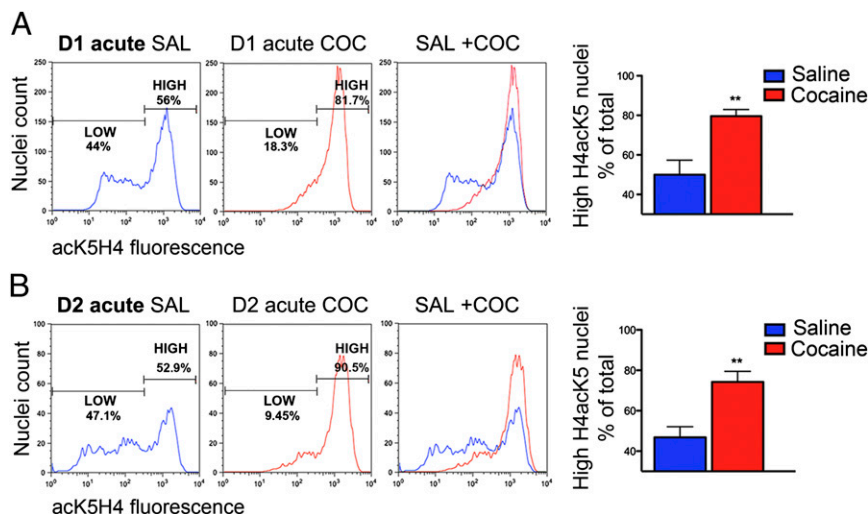


Fig. 5. Flow cytometry reveals the existence of subsets of D1 or D2 nuclei with different levels of histone H4 lysine-5 acetylation. AcK₅H4 immunofluorescence distribution in D1 (*A*) and D2 (*B*) nuclei 15 min after a single cocaine injection (20 mg/kg). For each condition, representative examples of flow cytometry plots of acK₅H4 immunofluorescence intensity in saline-treated (blue line, *Left*), cocaine-treated (red line, *Center*), or the superimposition of the two plots (*Right*) are shown. On each row, the bar graph (*Right*) shows quantification of the percentage of total nuclei with high acK₅H4 fluorescence in saline and cocaine-treated mice. The separation of the two populations is indicated in the representative plots. Data are means + SEM (*n* = 8–12; ***P* < 0.01, Student *t* test).

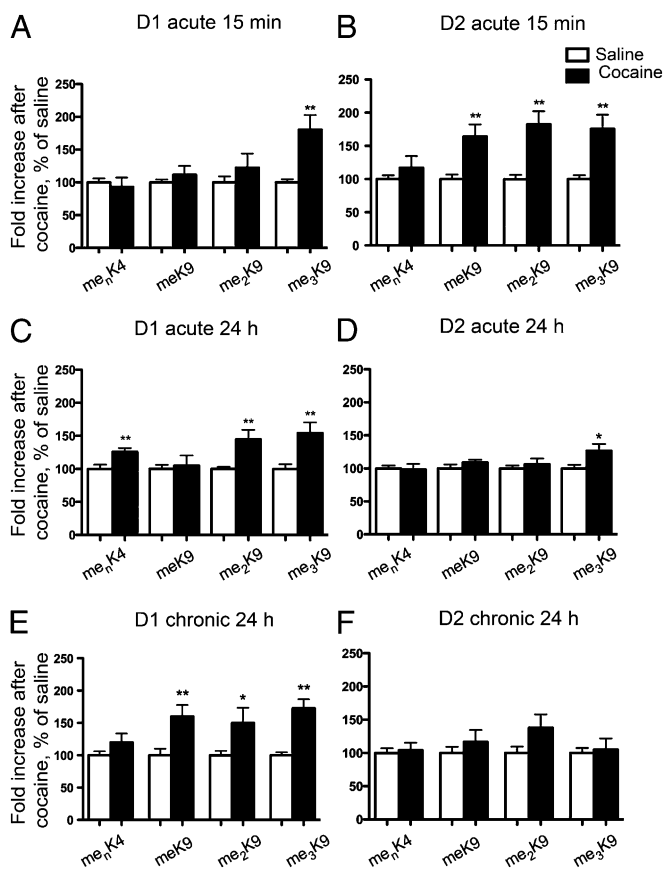


Fig. 6. Acute and chronic cocaine induce distinct patterns of histone H3 methylation in D1 or D2 nuclei. Flow cytometry analysis of H3 methyl-lysine4 (me_nK₄H3), H3 monomethyl-lysine9 (meK₉H3), H3 bimethyl-lysine9 (H3me₂K₉) and H3 trimethyl-lysine9 (H3me₃K₉) fluorescence in the GFP-positive nuclei from either D1 (A, C, and E) or D2 (B, D, and F) MSNs. EGFP-L10a mice were injected with saline or cocaine (20 mg/kg) and were killed after 15 min (A and B) or 24 h (C and D) later. Other mice received a daily injection of cocaine (20 mg/kg) or saline for 7 d and were killed 24 h after the last injection (E and F). Quantification of flow cytometry data are represented as percentage of change from saline control, mean + SEM ($n = 8-14$; * $P < 0.05$, ** $P < 0.01$, Student t test).

adult neurons are particularly problematic to study labile posttranslational modifications and introduce a risk of artifactual changes or lack of response. To overcome these limitations, we took advantage of a recently developed method (22) that used FACS to purify the nuclei of identified neuronal populations and study DNA methylation. A similar methodology has been used for chromatin immunoprecipitation (35, 36). Here we developed a unique approach using immunolabeling and flow cytometry of nuclei to obtain information about the dynamics of histone PTMs induced by cocaine in the two striatal MSN subtypes. We first compared the results obtained for two previously characterized histone modifications, pS₁₀H3 and pS₁₀K₁₄H3, with this method and those obtained by sorting followed by immunoblotting. This comparison validated the nuclear cytometry approach, which is faster and requires less material, allowing further characterization of histone PTMs.

Among the acetylated residues analyzed, acK₅H4 was the most dramatically altered: K₅ acetylation was increased in D1 nuclei in all cocaine treatment conditions. In contrast, in D2 nuclei it was increased 15 min after the first injection and unaltered 24 h after the last injection. AcK₁₄H3 was activated in D1 exclusively 15 min following a single injection, whereas it was activated only in D2 nuclei in chronically treated mice. Additional differences were noted for acetylation of H4 on K₈ and K₁₂. AcK₅H4 and to

a lesser degree acK₈H4 were persistent marks that increased in D1 neurons 24 h after single or repeated cocaine injections, in agreement with a previous report (37). It is important to note that the turnover of most acetyl groups is usually high, with reported half-lives of a few minutes (38). The apparent stability of some acetylation *in vivo* is therefore likely to result from changes in steady-state levels of acetylation, i.e., from stable changes in acetylation and/or deacetylation rates.

Histone acetylation is controlled by deacetylases (HDACs) and acetyltransferases (HATs), which have a broad range of specificity, with multiple enzyme isoforms being able to target the same residues. Acetylation of H4 K₅ and H4 K₁₂ is increased in the hippocampus of HDAC2 knock-out mice (39), suggesting the possible role of HDAC2 in the regulation of these residues. Interestingly, HDAC isoform expression has been found to be differentially modulated in D1 and D2 neurons after cocaine (21) and could explain the differential regulation of H4 acetylation. For instance, HDAC4 expression is increased by about 45% specifically in D2 neurons after chronic cocaine, possibly contributing to the observed decrease in H4 K₅ and K₁₂ acetylation. Moreover, chronic cocaine up-regulates the class III HDACs, sirtuins, in the NAc (25), although it is not known in which cell type. The functional role of histone acetylation is also indicated by the ability of an HDAC3 inhibitor to enhance extinction of cocaine-induced conditioned place preference, while promoting memory in an object recognition task (40).

Flow cytometry allowed the separation of two populations of neurons with high and low acK₅H4 immunofluorescence in both D1 and D2 MSNs. This bimodal distribution was not observed for all PTMs. The distribution of pS₁₀H3 or pS₁₀acK₁₄H3 immunoreactivity was unimodal in basal conditions (Fig. 2) and the distribution of fluorescence for other acetylated or methylated marks was variable. Cocaine administration shifted the low acK₅H4 immunofluorescence population toward the levels of immunoreactivity of the high fluorescence population, without increasing the latter. These data suggest the existence of distinct populations of nuclei in terms of K₅H4 acetylation level, sensitive to cocaine regulation.

Methylation marks are generally considered to be relatively stable, with a slower turnover than phosphorylation and acetylation and half-lives of 7–24 h (38). Nevertheless, we observed a rapid increase in methylation as early as 15 min after a single cocaine injection, suggesting that this PTM is as reactive as the others. D1 and D2 nuclei displayed contrasted profiles of histone methylation change after acute and chronic cocaine. Previous reports showed that a single exposure to cocaine increases the three methylated forms of H3 K₉ in the NAc (13, 29). Interestingly, 15 min after a single cocaine injection we found an increase of these modifications, which was most pronounced for the three forms in D2 nuclei, as well as for me₃K₉H3 in D1 nuclei. The differences between meK₉H3 and me₂K₉H3 versus me₃K₉H3 highlight the independent regulation of these modifications. Methylation steady state is controlled through the action of methyltransferases and demethylases. The heteromeric methyl transferase G9a/GLP, associating G9a and G9a-like protein (GLP), specifically generates meK₉H3 and me₂K₉H3, whereas me₃K₉H3 is produced by Suv39h, the murine homologue of *Drosophila* suppressor of variegation 3-9 (41). Our results are compatible with activation of Suv39h in both D1 and D2 MSNs and of G9a/GLP only in D2 MSNs. Suv39h is up-regulated in the total striatum after chronic amphetamine (12), but at the earliest investigated time point (15 min) its regulation is unlikely to result from changes in expression levels, but is more probably due to posttranslational mechanisms. In contrast, repeated injections of cocaine have been shown to down-regulate G9a expression in the NAc, but not Suv39h, via the transcription factor Δ FosB (truncated form of the FBJ murine osteosarcoma viral oncogene homologue B), which is induced in D1 neurons. However, we observed an increase in all three methylated forms of H3 K₉ in D1 but not in D2 neurons, suggesting the existence of other regulations. Differential regulation in D1 and D2 nuclei may explain apparent contradictions in the

literature. For example, chronic cocaine increases me₂K₉/K₂₇H3 associated with the majority of the genes studied (25), whereas a global decrease in me₂K₉H3 was reported (13). This underlines the importance of studying histone PTMs in specific cellular populations. It should also be kept in mind that our data were obtained from the whole striatum, including both caudate-putamen and accumbens. Different types of regulations in these two regions may explain some differences with previous reports focusing on the accumbens (13, 29).

Our method combining sorting and flow cytometry analysis of nuclei provides a unique assessment of the specific regulations of histone PTMs in the two populations of striatal MSNs. It shows the specificity, time dependence, and persistence of these modifications. Thus, it provides a strong framework to characterize the epigenetic changes and better understand the short-term and long-lasting regulations of transcription in the two neuronal populations, in the physiology of the basal ganglia and the long-term actions of drugs of abuse. Moreover it is a multipurpose method, which has the potential to be applied to any other genetically labeled cell types.

Experimental Procedures

Drd1a::EGFP-L10a and *Drd2::EGFP-L10a* bacTRAP lines that express the transgene EGFP-L10a were generated as described (21) and were maintained on a C57BL/6J background. Using similar transgenes, it was shown that virtually all D1R-expressing striatal cells are MSNs, whereas D2R-expressing cells are mostly MSNs but include also the much less abundant cholinergic interneurons (20). Mice received either one i.p. injection of 20 mg/kg cocaine-HCl (Sigma) or saline ("acute" regimen) and were killed by decapitation 15 min or 24 h after this single injection, or one daily injection of cocaine-HCl or saline for 7 consecutive days and were killed 24 h after the last injection (chronic regimen). The mouse head was dipped in liquid nitrogen for 5 s immediately after decapitation, the brain was removed, and the striata were rapidly dissected on a piece of dry ice before being

homogenized and subjected to nuclear fractionation. Animal procedures were performed in accordance with the National Institutes of Health *Guide for the Care and Use of Laboratory Animals* and were approved by The Rockefeller University Institutional Animal Care and Use Committee or in accordance with the guidelines of the French Agriculture and Forestry Ministry for handling animals (decree 87-848) under the approval of the "Direction Départementale de la Protection des Populations de Paris" (authorization C-75-828, license B75-05-22).

Nuclear fractionation and sorting were performed as described (22) with some modifications (*SI Experimental Procedures*). For flow cytometry analysis, striatal nuclei (about 500,000) from each animal were permeabilized, blocked, and aliquoted for single labeling with antibodies targeting histone posttranslational modifications. Control samples were incubated with the appropriate isotype antibody. After washing in PBS, nuclei were sequentially incubated with the secondary antibodies and Hoechst 33342 fluorescent DNA stain. Multiparameter analyses of stained nuclear suspensions were performed on the LSR II (BD) and analyzed with FlowJo software (Tree Star). Histone PTM indirect fluorescence was quantified using the geometric mean of fluorescence of the appropriate channel and expressed as a ratio to the mean isotype control fluorescence. The data were normalized in each experiment by expression as a percentage of the mean value in saline-treated mice.

Reagent sources, details of these experimental procedures, and the other procedures are described in *SI Experimental Procedures*.

ACKNOWLEDGMENTS. We thank Hugo Mouquet for methodological advice and Svetlana Mazel, Joel Cohen-Solal, Selamawit Tadesse, Xiao Li, and Stanka Semova from The Rockefeller University Flow Cytometry Resource Center. This work was supported by Fondation pour la Recherche Médicale and European Research Council (J.-A.G.), Department of Defense/US Army Medical Research Acquisition Activity Grants W81XWH-09-1-0108 and W81XWH-09-1-0402 (to P. Greengard), National Institutes of Health Grants DA10044 and MH90963 (to A.C.N. and P. Greengard), and the JPB Foundation (M.H. and P. Greengard). P. Guernonprez is a Centre National de la Recherche Scientifique Investigator.

1. Deroche-Gamonet V, Belin D, Piazza PV (2004) Evidence for addiction-like behavior in the rat. *Science* 305(5686):1014–1017.
2. Di Chiara G, Imperato A (1988) Drugs abused by humans preferentially increase synaptic dopamine concentrations in the mesolimbic system of freely moving rats. *Proc Natl Acad Sci USA* 85(14):5274–5278.
3. Koob GF, Le Moal M (2001) Drug addiction, dysregulation of reward, and allostasis. *Neuropsychopharmacology* 24(2):97–129.
4. Wise RA (2002) Brain reward circuitry: Insights from unsensed incentives. *Neuron* 36(2):229–240.
5. Berke JD, Hyman SE (2000) Addiction, dopamine, and the molecular mechanisms of memory. *Neuron* 25(3):515–532.
6. Badiani A, Belin D, Epstein D, Calu D, Shaham Y (2011) Opiate versus psychostimulant addiction: the differences do matter. *Nat Rev Neurosci* 12(11):685–700.
7. Kalivas PW (2004) Recent understanding in the mechanisms of addiction. *Curr Psychiatry Rep* 6(5):347–351.
8. Hyman SE, Malenka RC (2001) Addiction and the brain: The neurobiology of compulsion and its persistence. *Nat Rev Neurosci* 2(10):695–703.
9. Nantwi KD, Schoener EP (1993) Cocaine and dopaminergic actions in rat neostriatum. *Neuropharmacology* 32(8):807–817.
10. Dietz DM, Dietz KC, Nestler EJ, Russo SJ (2009) Molecular mechanisms of psychostimulant-induced structural plasticity. *Pharmacopsychiatry* 42(Suppl 1):S69–S78.
11. Borrelli E, Nestler EJ, Allis CD, Sassone-Corsi P (2008) Decoding the epigenetic language of neuronal plasticity. *Neuron* 60(6):961–974.
12. Renthall W, et al. (2008) Delta FosB mediates epigenetic desensitization of the c-fos gene after chronic amphetamine exposure. *J Neurosci* 28(29):7344–7349.
13. Maze I, et al. (2010) Essential role of the histone methyltransferase G9a in cocaine-induced plasticity. *Science* 327(5962):213–216.
14. Brami-Cherrier K, et al. (2005) Parsing molecular and behavioral effects of cocaine in mitogen- and stress-activated protein kinase-1-deficient mice. *J Neurosci* 25(49):11444–11454.
15. Robison AJ, Nestler EJ (2011) Transcriptional and epigenetic mechanisms of addiction. *Nat Rev Neurosci* 12(11):623–637.
16. Lobo MK, Nestler EJ (2011) The striatal balancing act in drug addiction: Distinct roles of direct and indirect pathway medium spiny neurons. *Front Neuroanat* 5:41.
17. Valjent E, Bertran-Gonzalez J, Hervé D, Fisone G, Girault JA (2009) Looking BAC at striatal signaling: cell-specific analysis in new transgenic mice. *Trends Neurosci* 32(10):538–547.
18. Gerfen CR (1992) The neostriatal mosaic: Multiple levels of compartmental organization in the basal ganglia. *Annu Rev Neurosci* 15:285–320.
19. Bateup HS, et al. (2008) Cell type-specific regulation of DARPP-32 phosphorylation by psychostimulant and antipsychotic drugs. *Nat Neurosci* 11(8):932–939.
20. Bertran-Gonzalez J, et al. (2008) Opposing patterns of signaling activation in dopamine D1 and D2 receptor-expressing striatal neurons in response to cocaine and haloperidol. *J Neurosci* 28(22):5671–5685.
21. Heiman M, et al. (2008) A translational profiling approach for the molecular characterization of CNS cell types. *Cell* 135(4):738–748.
22. Kriaucionis S, Heintz N (2009) The nuclear DNA base 5-hydroxymethylcytosine is present in Purkinje neurons and the brain. *Science* 324(5929):929–930.
23. Kumar A, et al. (2005) Chromatin remodeling is a key mechanism underlying cocaine-induced plasticity in striatum. *Neuron* 48(2):303–314.
24. Levine AA, et al. (2005) CREB-binding protein controls response to cocaine by acetylating histones at the fosB promoter in the mouse striatum. *Proc Natl Acad Sci USA* 102(52):19186–19191.
25. Renthall W, et al. (2009) Genome-wide analysis of chromatin regulation by cocaine reveals a role for sirtuins. *Neuron* 62(3):335–348.
26. Cheung P, Allis CD, Sassone-Corsi P (2000) Signaling to chromatin through histone modifications. *Cell* 103(2):263–271.
27. Maze I, Nestler EJ (2011) The epigenetic landscape of addiction. *Ann N Y Acad Sci* 1216:99–113.
28. Barski A, et al. (2007) High-resolution profiling of histone methylations in the human genome. *Cell* 129(4):823–837.
29. Maze I, et al. (2011) Cocaine dynamically regulates heterochromatin and repetitive element silencing in nucleus accumbens. *Proc Natl Acad Sci USA* 108(7):3035–3040.
30. Wolf ME, Kapatos G (1989) Flow cytometric analysis and isolation of permeabilized dopamine nerve terminals from rat striatum. *J Neurosci* 9(1):106–114.
31. Arlotta P, et al. (2005) Neuronal subtype-specific genes that control corticospinal motor neuron development in vivo. *Neuron* 45(2):207–221.
32. St John PA, Kell WM, Mazzetta JS, Lange GD, Barker JL (1986) Analysis and isolation of embryonic mammalian neurons by fluorescence-activated cell sorting. *J Neurosci* 6(5):1492–1512.
33. Guez-Barber D, et al. (2011) FACS identifies unique cocaine-induced gene regulation in selectively activated adult striatal neurons. *J Neurosci* 31(11):4251–4259.
34. Lobo MK, Karsten SL, Gray M, Geschwind DH, Yang XW (2006) FACS-array profiling of striatal projection neuron subtypes in juvenile and adult mouse brains. *Nat Neurosci* 9(3):443–452.
35. Bonn S, et al. (2012) Cell type-specific chromatin immunoprecipitation from multicellular complex samples using BiTS-ChIP. *Nat Protoc* 7(5):978–994.
36. Jiang Y, Matevosian A, Huang HS, Straubhaar J, Akbarian S (2008) Isolation of neuronal chromatin from brain tissue. *BMC Neurosci* 9:42.
37. Martin TA, et al. (2012) Methamphetamine causes differential alterations in gene expression and patterns of histone acetylation/hypoacetylation in the rat nucleus accumbens. *PLoS ONE* 7(3):e34236.
38. Barth TK, Imhof A (2010) Fast signals and slow marks: The dynamics of histone modifications. *Trends Biochem Sci* 35(11):618–626.
39. Guan JS, et al. (2009) HDAC2 negatively regulates memory formation and synaptic plasticity. *Nature* 459(7243):55–60.
40. Malvaez M, et al. (2013) HDAC3-selective inhibitor enhances extinction of cocaine-seeking behavior in a persistent manner. *Proc Natl Acad Sci USA* 110(7):2647–2652.
41. Lachner M, O'Sullivan RJ, Jenuwein T (2003) An epigenetic road map for histone lysine methylation. *J Cell Sci* 116(Pt 11):2117–2124.